Research Square

Preprints are preliminary reports that have not undergone peer review.
They should not be considered conclusive, used to inform clinical practice,
or referenced by the media as validated information.

ADAR1-dependent miR-3144-3p editing simultaneously induces MSI2 and suppresses SLC38A4 in liver cancer

Suk Woo Nam (swnam@catholic.ac.kr)
The Catholic University of Korea
Hyung Seok Kim
The Catholic University of Korea
Min Jeong Na
The Catholic University of Korea
Keun Hong Son
Dankook University
Hee Doo Yang
The Catholic University of Korea
Sang Yean Kim
The Catholic University of Korea
Eunbi Shin
The Catholic University of Korea
Jin Woong Ha
The Catholic University of Korea
Soyoung Jeon
The Catholic University of Korea
Keunsoo Kang
Dankook University
Kiho Moon
Neornat Inc.
Won Sang Park
Catholic University of Korea https://orcid.org/0000-0002-9090-0584

Article

Keywords: ADAR1, RNA editing, miR-3144-3p, MSI2, SLC38A4

Posted Date: September 28th, 2022

DOI: https://doi.org/10.21203/rs.3.rs-1999877/v1

License: This work is licensed under a Creative Commons Attribution 4.0 International License.
Read Full License

Version of Record: A version of this preprint was published at Experimental & Molecular Medicine on January 4th, 2023. See the published version at https://doi.org/10.1038/s12276-022-00916-8.

Abstract

Aberrant adenosine-to-inosine (A-to-I) RNA editing, catalyzed by adenosine deaminase acting on double-stranded RNA (ADAR), is implicated in various cancers, but the mechanisms by which microRNA (miRNA) editing contributes to cancer development are currently largely unknown. Our multi-step hepatocellular carcinogenesis transcriptome data analyses, together with publicly available data, indicated that *ADAR1* is the most dysregulated gene among the RNA editing enzyme families in liver cancer. Targeted inactivation of *ADAR1* inhibits *in vitro* tumorigenesis of liver cancer cells. Integrative computational analyses of RNA editing hotspots and the editing frequency of miRNAs suggested miR-3144-3p a potential mRNA edited by ADAR1 in liver cancer progression. ADAR1 promoted A-to-I editing of the canonical miR-3144-3p to change position 3 adenosine in the seed region to guanine (ED_miR-3144-3p(3_A < G)) in liver cancer cells. We then demonstrated that *Musashi RNA-binding protein 2* (*MSI2*) is a specific target of miR-3144-3p, and that MSI2 overexpression is due to ADAR1-dependent over-editing of the canonical miR-3144-3p in liver cancer. In addition, target prediction analyses and validation experiments identified *solute carrier family 38 member 4* (*SLC38A4*) as specific target gene for ED_miR-3144-3p(3_A < G). Ectopic expressions of both ADAR1 and ED_miR-3144-3p(3_A < G) mimics enhanced mitotic activities and that ADAR1 suppressed SLC38A4 in liver cancer cells. Treatments with mouse-specific ADAR1-, MSI2-siRNA or SLC39A4-expressing plasmids suppressed tumor incidence and growth in a spontaneous mouse liver cancer model. Our findings suggest that aberrant regulation of ADAR1 augments oncogenic MSI2 via overediting the canonical miR-3144-3p, and the resultant ED_miR-3144-3p(3_A < G) simultaneously suppresses tumor suppressor SLC38A4, thereby contributing to hepatocellular carcinogenesis.

Introduction

In cellular biology, the epitranscriptome comprises post-transcriptional RNA modifications, including methylation, splicing and RNA editing, that lead to various functional changes of the transcriptome.[1] Among these, RNA editing is a widespread co- or post-transcriptional modification process that introduces changes in RNA sequences encoded by the genome, and contributes to RNA mutations.[1,2] The best characterized examples of RNA editing in mammals are the conversion of cytosine to uracil (C-to-U) and adenosine to inosine (A-to-I).[3] In humans, the most frequent type of RNA editing is the conversion of A-to-I, which is catalyzed by the double-stranded-RNA (dsRNA)-specific adenosine deaminase acting on RNA (ADAR) family of proteins, composed of ADAR1, ADAR2 and ADAR3, all of which contain dsRNA-binding domains.[4]

In general, as a result of RNA editing, inosine bases are interpreted by the cellular machinery as guanosine, and are base-pared with cytosine, making the presence of A-to-I similar to an A-to-G substitution. Such changes can lead to specific amino acid substitutions, alternative splicing, microRNA (miRNA)-mediated gene silencing, and/or changes in transcript localization and stability. Aberrant RNA editing is an underexplored mechanism to reproducibly alter protein and regulatory RNA sequences,

acting as a driver of carcinogenesis, and therefore, a potential therapeutic target.[5] Indeed, A-to-I editing and the enzymes mediating modification are significantly altered in cancer. In most tumor types, editing activity is elevated when compared with matched normal tissues, but some cancers are reported to be underedited.[6] The vast majority of A-to-I RNA editing events occur in non-coding regions, such as untranslated regions (UTRs), introns, long non-coding RNAs and miRNAs. In addition, systematic characterization of A-to-I editing hotspots in miRNAs across many types of human cancer have suggested the importance of miRNA editing in gene regulation and its potential as a biomarker for cancer prognosis and therapy.[7]

The editing of RNA with in miRNAs has the potential to regulate the processing of precursor miRNAs into mature miRNAs.[8] Also, A-to-I editing of primary miRNA forms by ADARs interferes with miRNA biogenesis and thereby alters miRNA homeostasis. Moreover, because miRNA regulation requires perfect base-pairing within the seed region (2 ~ 8 positions) of miRNA, a single nucleotide change can alter miRNA target recognition.[9] Given a single nucleotide change can alter the base pairing properties of miRNA, editing within the seed sequence of miRNA could alter recognition of target genes by deleting the original targets or acquiring new targets. Intriguingly, several miRNA editing events appear to be critical in cancer. For example, edited miR-455 is postulated to suppress tumor growth and metastasis by up-regulating tumor suppressor *CPEB1* in melanoma.[10] In contrast, a recent study reported that ADAR1-mediated miR-200b overediting contributed to thyroid cancer.[11] On the other hand, it has been reported that aberrant editing of mRNAs for specific genes, such as *AZIN1*, *FLNB* and *COPA*, contributed to the development of liver cancer,[12] but ADAR-dependent editing of non-coding RNA remains to be studied.

Here, we investigated the oncogenic function of ADAR1 by promoting miR-3144-3p editing to simultaneously induce *Musashi RNA-binding protein 2* (*MSI2*) and suppress *solute carrier family 38 member 4* (*SLC38A4*) in human liver cancer. We explored transcriptome and small-RNA-sequencing data for human multi-stage liver disease including chronic hepatitis, cirrhosis, dysplastic nodule and liver cancers. From this, ADAR1 was suggested to be overexpressed among the RNA editing enzyme family, and miR-3144-3p was identified as an ADAR1 editing target in liver cancer. We then showed that ADAR1 overexpression and consequent miR-3144-3p editing augment the aggressiveness of liver cancer cells through their effects on growth, proliferation, invasion, migration and *in vivo* tumor growth. Notably, we demonstrated that ADAR1 promotes miR-3144-3p overediting, especially adenine position 3 in the sequence of the canonical miR-3144-3p seed region, to produce guanine-changed miR-3144-3p (ED_miR-3144(3_A < G) in liver cancer cells. This critical ADAR1-dependent change in the canonical miR-3144-3p seed region attenuated negative regulation of canonical miR-3144-3p activity on *MSI2* mRNA, and simultaneously created a novel edited miRNA, ED_miR-3144(3_A < G), that inhibits mRNA translation of tumor suppressor *SLC38A4* in liver cancer cells. Our study identified the pathogenic activity of ADAR1-mediated miRNA editing to suppress canonical miRNA activity and create edited miRNA that potentiates malignant transformation and growth of hepatocytes.

Materials And Methods

Tissue samples

A total of 36 matched pairs of liver cancer tissues and their corresponding noncancerous liver tissues were obtained from AJOU University Hospital and Keimyung University Hospital, a member of National Biobank of Korea. Written informed consent was obtained from each subject according to the Declaration of Helsinki, and the study was approved by the Institutional Review of Board (IRB) of the Songeui Campus, College of Medicine, the Catholic University of Korea (IRB approval number: MC18TESI0075, MC19TESI0016).

Cell culture

Human liver cancer cells (Hep3B, HepG2, Huh7, PLC/PRF/5, SK-HEP-1, SNU-182, SNU-354, SNU-368, SNU-387, SNU-423, SNU449, and SNU-475) were obtained from KCLB (Korean Cell Line Bank, Seoul, Korea). Normal liver cell line MIHA was kindly provided by Dr. Roy-Chowdhury (Albert Einstein College of Medicine, Bronx, NY). All of the cell lines were held in an RPMI-1640 or DMEM medium with 10% fetal bovine serum added and 100 units/ml of penicillin/streptomycin (GenDepot, Katy, TX). All cells were cultured at 37°C in a humidified incubator with 5% CO2.

Transfection and treatment

Small interfering RNAs (siRNAs) were synthesized by Genolution (Seoul, Korea) or purchased from BIONEER (Daejeon, Korea). The sequences of the siRNAs, miRNA mimics and antisense miRNAs are listed in Supplementary data, Table S5. Human ADAR1-p110, MSI2 and SLC38A4 expression plasmid, subcloning gene ORF sequence in pcDNA3.1+/C-(K)-DYK plasmid, was purchased from Genscript™ (Piscataway, NJ, USA). Transfections were carried out using Lipofectamine RNAiMAX or Lipofectamine 2000 reagent (Invitrogen, Carlsbad, CA, USA), according to the manufacturer's instructions.

RNA, DNA extraction, RT-PCR and qRT-PCR

Total RNA from frozen tissues and cells were isolated using Trizol reagent (Invitrogen, Carlsbad, CA, USA). One microgram of total RNA was reverse transcribed into cDNA using Tetro cDNA Synthesis Kit (Bioline, London, UK) according to the manufacturer's instructions. The quantitative real-time PCR (qRT-PCR) were performed with SensiFAST SYBR No-ROX Kit (Bioline, London, UK) and monitored in real-time by an iQ™-5 (Bio-Rad, Hercules, CA, USA). The average threshold cycle (Ct) value, from triplicate assays were used for further calculations. Normalized gene expression was determined using the relative quantification method. Results were expressed as the mean value of triplicate experiments. Genomic DNA from tissue and cells were isolated using DNAzol reagent (Invitrogen, Carlsbad, CA, USA), according to the manual. qRT-PCR was performed as described above and glyceraldehyde-3-phosphate dehydrogenase (GAPDH) was used as endogenous loading control. The sequences of primers used in qRT-PCR are listed in Supplementary data, Table S6.

FLAG immunoprecipitation

Cells were transfected with pcDNA3.1_ADAR1-p110 or pcDNA3.1_MSI2, which encodes a FLAG-tag. 48 hr after transfection, the cells were washed with phosphate-buffered saline (PBS) and lysed at 4°C in PBS, pH 7.2, containing 1.0% NP-40, 0.5% sodium deoxycholate, 0.1% SDS, 10mM NaF, 1.0 mM NaVO4, and 1.0% protease inhibitor cocktail (Sigma). The FLAG tag was immunoprecipitated with anti-FLAG DynaBeads (Invitrogen, Carlsbad, CA) during an overnight incubation. Immunoprecipitated proteins were eluted using 3X FLAG peptide (Sigma) and analyzed by Western blot, probing with anti-FLAG antibody (Cell Signaling). For primary-mir-3144 pulldown analysis using qRT-PCR, RNA was isolated and reverse-transcribed using a miScript II RT kit (Qiagen).

Western blot analysis

Cells were lysed using a lysis buffer (50 mM HEPES, 5 mM EDTA, 50 mM NaCl, 1% Triton X100, 50 mM NaF, 10 mM Na2P4O7, 1 mM Na3VO4, 5 ug/mL aprotinin, 5 ug/mL leupeptin, 1 mM PMSF and protease inhibitor cocktail). Lysates containing equal amounts of proteins were separated by SDS-PAGE and transferred onto a polyvinylidene difluoride membrane (Bio-Rad, Hercules, CA, USA). The blots were blocked with a 5% skim milk solution and incubated with the following antibodies: anti-ADAR1, anti-CTNNB1, anti-GAPDH, anti-MSI2, anti-MET, and anti-SLC38A4 (Santa Cruz Biotechnology, Dallas, TX, USA), and anti-Flag-Tag (Cell Signaling Technology, Danvers, MA, USA). The Immobilon™ western blot detection system (Millipore) was used to detect bound antibodies. The intensities of the western blot bands were quantified using LAS-4000 (Fuji Photo Film Co., Tokyo, Japan).

Cell growth assay

Cells were seeded in a 6-well plate for transfection. After transfection, cells were incubated with 0.5 mg/ml of MTT [3-(4,5-dimethylthiazol-2-yl)-2,5-diphenyltetrazolium bromide] solution (Sigma) for 1 hr. The dark blue formazan products formed by viable cells were dissolved in dimethyl sulfoxide (DMSO; Sigma), and absorbance was measured using a VICTOR3 Multilabel plate reader (PerkinElmer, Waltham, MA).

Bromodeoxyuridine (BrdU) incorporation assay

Cells were seeded in a 24-well plate to 40% ~ 50% confluency. The assay was performed with a Bromodeoxyuridine (BrdU) cell proliferation assay kit (Millipore) in accordance with the manufacturer's protocol every 24 hr.

Clonogenic assay

Cells were transfected with miRNA mimics or siRNA in 60 mm2 cell culture plates. After transfection for 24 hr, cells were re-seeded in 6-well plates and incubated for 2 weeks. Next, cells were washed with PBS and fixed with 1% paraformaldehyde for 30 min at room temperature. Fixed cells were stained with 0.5% crystal violet for 1 hr at room temperature. Colonies were counted using a clono-counter program.

Apoptosis assay

To measure levels of apoptosis, Annexin V-FITC Apoptosis Detection Kit I (BD Biosciences, San Jose, CA) was used. After transfection, liver cancer cells were washed with cold phosphate buffered saline (PBS) and resuspended in 1× binding buffer. Then, 1×10^5 cells were transferred to a 5 ml culture tube and mixed with 5 μl of annexin V-FITC and 10 ul of propidium iodide solution. After 20 min at room temperature in the dark, 400 μl of 1X binding buffer was added to each tube, and apoptotic fractions were measured by a FACS Calibur flow cytometer (BD Biosciences).

Cell cycle analysis

Liver cancer cells were transfected with miRNA mimics or siRNA in 60 mm dishes. After 48 h incubation, cells were harvested Trypsin, washed with cold PBS, fixed in 70% ethanol, resuspended in 200 ul PBS containing 1 mg/ml RNase and incubated in the dark for 30 min at 37o C. Nuclei were stained with 50 ug/ml propidium iodide (BD Biosciences). Stained cells fractions were measured using Cell-Quest FACS analysis software (BD Biosciences).

Migration and invasion assay

For in vitro cell migration and invasion assay, cell motility was measured by using a modified Boyden chamber assay. For invasion assay, Matrigel (BD Biosciences) was diluted to a concentration of 0.3 mg/ml with coating buffer. One hundred microliter aliquots of Matrigel were used to coat the upper surface of the Transwell cell culture inserts. After incubation for 2 h at 37°C, the inserts were ready to be seeded with cells. After preparation, cells were plated on the top surfaces of Transwell inserts, and the inserts were placed in a 24-well plate. The lower wells contained 2% FBS as a chemoattractant. The plate was incubated overnight and stained using a Diff-Quik staining kit (Sysmex, Kobe, Japan). The cell images were captured using an Axiovert 200 inverted microscope (Zeiss, Oberkochen, Germany) at × 200 magnification, and the number of cells was counted in three random image fields.

Wound healing assay

Cells were transfected and incubated for 24 hr in 60 mm^2 cell culture plates. Then, cells were trypsinized, and 1 × 10^6 cells per well were seeded in a 6-well cell culture plate. After overnight incubation, cell monolayers were scraped with a sterile micropipette tip. Initial gap widths 0 hr after scratching and residual gap widths 24 hr after scratching were photographed using an IX71 photomicrograph (Olympus, Tokyo, Japan).

Mutagenesis

For mutagenesis of ADAR1-p110 adenosine deaminase activity, a QuickChange kit (Agilent Technologies, Palo Alto, CA, USA) was used according to the manufacturer's instruction.

Mouse liver cancer model

The H-*ras* homozygous transgenic mice were kindly provided by Dr. Dae-Yeoul Yu (Laboratory of Human Genomics, Korea Research Institute of Bioscience and Biotechnology, Daejeon, Korea).[13] Male mice spontaneously developed liver cancer beginning at approximately 15–18 weeks of age. Mouse livers

were harvested at 24 weeks of age, and processed for the experiments. All procedure of animal research were provided in accordance with the Laboratory Animals Welfare Act, the Guide for Care and Use of Laboratory Animals and the Guidelines and Policies for Rodent experiment provided by the IACUC (Institutional Animal Care and Use Committee) in school of medicine, The Catholic University of Korea. (Approval number: CUMS-2019-0115-02)

Mfuzz clustering

The gene expression profiles were log-normalized and clustered using the c-mean algorithm by the Bioconductor Mfuzz package v. 2.30.0 as indicated by the author.[14]

Analyses of publicly available genomic data

To investigate differential gene expression of coding and non-coding RNAs in multi-stage liver disease, data were obtained from 'The Cancer Genome Atlas' liver cancer project (TCGA_LIHC), the International Cancer Genome Consortium liver Cancer–RIKEN, JP (ICGC_LIRI) and the Gene Expression Omnibus (GEO) database of the National Center for Biotechnology Information (NCBI) (Accession Numbers: GSE6764, GSE77314, GSE114564 and GSE174608). Level 3 mRNA expression data from TCGA-LIHC HTSeq-FPKM were log2 transformed [log2(fpkm + 1)] and used to assess gene expression.

MicroRNA target prediction

An *in silico* analysis was conducted to predict target candidates of miR-3144-3p and ED_miR-3144(3_A < G) by using the TargetScan algorithm (http://www.targetscan.org/). The sequence information of miR-3144-3p was obtained from miRbase database (http://www.mirbase.org).

Analysis of miRNA A-to-I editing using the catholic_mLIHC and TCGA_LIHC datasets

All bam files were converted to fastq format using bedtools bamtofastq. To remove adaptors, and low-quality and inadequate-length reads from the our human multi-stage liver cancer transcriptome data (Catholic_mLIHC) and TCGA_LIHC data, Cutadapt was used with the "-a adaptor_sequence –quality-base 33 -m 15 -M 28 -f fastq -O 3 -q 20" options. Next, Bowtie was used to align the filtered read to the human genome (hg19) with the "-n 1 –e 50 –a –m –best –strata –trim3 2" option for the best alignment, one mismatch per read, and no cross mapping. In the miRNA editing profile stage, all procedures were performed using the scripts reported in Wang et al. [15] Briefly, first, the binomial test was performed, and only results with a Bonferroni-corrected *p*-value of 0.1 or less were selected. Second, all SNPs present on mitochondria and in sites other than pre-miRNA were removed. Finally, in order to exclude all SNPs already reported, all mutations overlapping with information recorded from the dbSNP and gnomAD were removed. To obtain more meaningful results, miRNAs with an average editing rate of 5% or more and a TPM expression value of 1 or more were selected for the Catholic_mLIHC, and miRNAs with an editing rate of 5% or more in at least 10 samples or more were selected in the TCGA_LIHC dataset.

In vivo **tumorigenesis study**

Ras-Tg mice were intravenously injected with Invivofectamine 3.0 (Invitrogen, Carlsbad, CA, USA) containing 0.25 mg/kg of Adar1 and Msi2 siRNAs as previously described.[16] Ras-Tg mice were also intravenously injected with 50 μg of pcDNA3.1_Slc38a4 using Turbofect *in vivo* Transfection Reagent (Invitrogen, Carlsbad, CA, USA). The ultrasonography images were taken at 17, 19, 21 and 23 weeks of age with an ultrasound machine (Philips, Amsterdam, Nederland) by the same medical imaging expert each time.

Statistical analyses

Survival curves were plotted using the Kaplan-Meier product limit method, and significant differences between survival curves were determined using the log-rank test. All experiments were performed at least three times, and all samples were analyzed in triplicate. The statistical significance of the difference between experimental groups was assessed by paired or unpaired Student's t tests using GraphPad 7.0 software (GraphPad Software Inc.). Statistical significance was determined for $p < 0.05$. A chi-square test (two-sided) was used to determine associations between parameters. Receiver operating characteristic (ROC) curves for each candidate marker were analyzed to calculate sensitivity, specificity, and areas under the curve (AUC) with 95% confidence intervals.

Results

Identification of ADAR1 as potential RNA editing factor in liver cancer

A previous study reported that aberrant RNA editing, especially A-to-I, is mediated by ADARs in human liver cancer, but the precise mechanism by which such editing contributes to liver cancer has not yet been identified.[17] Based on this report, we recapitulated differential expressions of RNA editing gene families of publicly available (TCGA_LIHC, ICGC_LIRI, and GSE77314) and our multi-stage liver cancer (Catholic_mLIHC; GSE114564) transcriptome data. We found *ADAR1* was significantly overexpressed in liver cancer patients ($\geq \pm 1.5$ fold, $P < 0.05$), and *APOBEC3B* was also significantly upregulated in the same data sets (Fig. 1A and Supplementary data, Table S1). However, comparative gene expression analyses of *ADAR1* and *APOBEC3B* using the multi-stage liver cancer data sets showed cancer-specific expression of *ADAR1* in liver cancer (Supplementary Figure S1A, B), and the ROC analysis also exhibited that *ADAR1* expression was more specific to liver cancer than *APOBEC3B* (Supplementary Figure S1C, D). Next, we investigated genetic alteration of *ADAR1* in TCGA datasets. Genomic amplification at the *ADAR1* locus occurred frequently (12.5%), and this genetic alteration was significantly correlated with *ADAR1* mRNA expression in liver cancer (Fig. 1B). The PCR-based copy number analysis of selected 36-matched pairs of human liver cancer tissues found alteration of 44% of *ADAR1* gene copies in liver cancer (gain (n = 7) and amplification (n = 9)) (Fig. 1C). Notably, *ADAR1* gene amplification and mutation of the *CTNNB1* gene encoding β-catenin protein B were mutually exclusive in liver cancer when examining the TCGA_LIHC dataset, which was found to be the highest (38.2%, n = 138) in the 32 cancer types investigated in TCGA Pan-Cancer Atlas, and this mutually exclusive tendency was occurred only in liver

cancer (Fig. 1D and Supplementary data, Table S2). In addition, in the Kaplan-Meier survival analysis of the TCGA_LIHC data for liver cancer patients, alterations of *ADAR1* and *CTNNB1* were associated with a poor prognosis than that for patients without such alterations (Fig. 1E). We then confirmed that 9 of 12 tested liver cancer cell lines exhibited ADAR1 overexpression in both western blot and qRT-PCR analyses as compared with MIHA, an immortalized non-transformed hepatocyte cell line (Supplementary Figure S2A, B). We also found that ADAR1 was highly expressed in liver cancer on western blot analyses, but β-catenin was not expressed in 10 liver cancer tissues (Fig. 1F).

Tumorigenic potential of ADAR1 and identification of miRNA editing in liver cancer

To identify the functional roles of ADAR1 in liver cancer, we performed *in vitro* tumorigenesis assays. We found ADAR1 knock-down significantly suppressed the growth and proliferation of the Hep3B and Huh7 cells (Fig. 2A, B). In addition, flow cytometry analyses indicated that ADAR1 knock-down significantly increased G1-arrest, but had no effect on cellular death processing in the same cells (Fig. 2C, D). Consistently, ADAR1 knock-down was correlated with anti-tumorigenic effects in scratch wound healing, *in vitro* motility and invasion assays (Fig. 2E, F).

Based on these results, we searched for miRNAs that are the target of ADAR1 editing in liver cancer. Among the miRNAs in which editing occurs, only miRNAs whose editing site is included in the miRNA seed region were selected from small-RNA sequencing data of both the Catholic_mLIHC and TCGA_LIHC datasets. Then, to identify the miRNAs that contained high-confidence RNA editing hotspots, miRNAs with A-to-I editing rates of 5% or more were selected. Finally, in Catholic_mLIHC datasets, miRNAs for which the editing frequency increased as liver cancer progressed were selected, and in TCGA_LIHC datasets, miRNAs for which the editing frequency increased in liver cancer as compared with normal tissue were selected. In this way, four miRNAs—miR-1304-3p, miR-3144-3p, miR-499a-3p and miR-589-3p—commonly included in both datasets were included in the finally analyses (Supplementary Figure S3A). Of these, miR-3144-3p was found to associated with A-to-I editing in the seed region, and it was also confirmed that the editing frequency increased as the liver cancer stage progressed and, at the same time, was statistically significantly increased compared with normal liver tissue (Supplementary Figure S3B, C). It was also noted that the editing frequency and level of miR-3144-3p increased as the *ADAR1* gene copy number increased (Supplementary Figure S3D).

Next, to confirm the editing event of miR-3144-3p in liver cancer patients, we searched editing sites of both full-length primary miRNA 3144 (mir-3144) and mature form of miR-3144 sequences in Catholic_mLIHC datasets. Notably, among the entire mir-3144 sequence, A-to-I (G) editing sites were identified only in the mature miR-3144-3p sequence, especially in the seed region and it was confirmed that these editing events increased as liver cancer progressed (Fig. 3A; Supplementary Figure S4A). Then, after ADAR1 knock-down in the Hep3B and Huh7 liver cancer cell lines, direct sequencing of the target site of the seed region resulted in an increase in the canonical form of adenine (A), together with a reduction in the edited form of guanine (G) (Fig. 3B). Next, to investigate whether the seed region of miR-3144-3p is

directly catalyzed by ADAR1, we prepared two different plasmids, pcDNA3.1_ADAR1-p110_wild (active functional form of ADAR1-p110 in liver cancer) and pcDNA3.1_ADAR1-p110_mutant (mutant form in adenine deaminase domain), respectively (Supplementary Figure S4B). We observed significant enrichment of primary mir-3144 when pcDNA3.1_ADAR1-p110_wild was transfected into the MIHA and SNU-449 cell line that have relatively low expression of ADAR1 (Fig. 3C). Direct sequencing of the major editing site in the seed region revealed that introducing enzymatically active ADAR1 (pcDNA3.1_ADAR1-p110_wild) induced the edited form of guanine (G), whereas the mutant form of ADAR1 (pcDNA3.1_ADAR1-p110_mutant) did not affect A-to-I (G) editing of the seed region of miR-3144-3p (Fig. 3D).

Identification of targets of canonical and edited miR-3144-3p in liver cancer

In liver cancer cells strongly expressing ADAR1, transfection with an miR-3144-3p mimic showed a significant growth inhibitory effect similar to that of ADAR1 knock-down, implying attenuation of canonical miR-3144-3p by ADAR1 editing (Fig. 4A). Since ADAR1 editing of miR-3144-3p occurs in the seed region, it induces the re-expression of the target regulated by canonical miR-3144-3p. To test this hypothesis, we identified targets of canonical miR-3144-3p using the target prediction program TargetScan (http://www.targetscan.org/). This integrated analysis strategy using Mfuzz and gene expression pattern analyses identified MSI2, STXBP4 and SUV39H as target candidate genes of canonical miR-3144-3p, (Supplementary Figure S5A, B; Supplementary data, Table S3). Among these candidates, only MSI2 was inhibited in both liver cancer cell lines (Supplementary Figure S6A, B).

In other experiments, ADAR1 editing of the canonical miR-3144-3p created a novel miRNA in which adenine at the position 3 of the seed region is changed to guanine (ED_miR-3144(3_A < G). Since the expression of the newly edited and generated ED_miR-3144(3_A < G) target gene is reduced as liver cancer progressed, five candidates, INMT, GHR, GLYAT, SLC38A4 and HMGCS2, were derived through target prediction and expression pattern analyses (Supplementary Figure S5C, D; Supplementary data, Table S3). When MIHA and SNU-449 cells were transfected with ED_miR-3144(3_A < G) mimic or pcDNA3.1_ADAR1-p110_wild in the presence of primary mir-3144, only the SLC38A4 candidate target gene was inhibited in both liver cancer cell lines (Supplementary Figure S6C, D). Therefore, we selected MSI2, Musashi RNA-binding protein, as a target for canonical miR-3144-3p and SLC38A4 (solute carrier family 38 member 4) as a target for edited ED_miR-3144(3_A < G) for additional functional studies in liver cancer.

First, the regulation of the canonical miR-3144-3p on MSI2 in liver cancer was confirmed. Ectopic expression of an miR-3144-3p mimic suppressed MSI2, whereas co-transfection of an antisense miR-3144-3p (AS-miR-3144-3p) mimic rescued this effect in liver cancer cells (Fig. 4B, upper). Note that an ED_miR-3144(3_A < G) mimic did not suppress MSI2 in either western blot or luciferase assays, implying the specific targeting of MSI2 by the canonical miR-3144-3p (Fig. 4B, middle and lower). In addition, ectopic expression of primary mir-3144-3p or ADAR1 knock-down significantly suppressed MSI2 in both

western bot and luciferase assays in the same cells (Fig. 4C). Notably, MSI2 suppression by ectopic expression of primary mir-3144 was rescued by pcDNA3.1_ADAR1-p110_wild, an active ADAR1, whereas the mutant form of ADAR1 had no effects on miR-3144 expression in the same cells (Fig. 4D).

Recently, MSI2 was reported to be a cancer driver gene, and was postulated to be a possible effector in the development of cancer.[18] We assessed differential expression of the effector genes in three large cohorts of liver cancer patients within the Catholic_mLIHC, TCGA_LIHC and ICGC_LIRI datasets (Supplementary data, Table S4). The analyses indicated *HMGA2*, *MKI67*, *HOXA9* and *MET* were significantly overexpressed in the above cohorts. Among these, only *MET* expression was found to be regulated by MSI2 in a qRT-PCR assay of liver cancer cells (Supplementary Figure S7A, B). We then used western blot analyses to confirm that when MSI2 was selectively suppressed, MET was also suppressed, and conversely, when MSI2 was overexpressed, the expression of MET was also increased in liver cancer cells (Fig. 4E). Finally, MET was found to be significantly enriched as a result of knocking down intracellular MSI2 after overexpression of MSI2 in liver cancer cells (Fig. 4F). These results indicated that aberrant expression of ADAR1 in liver cancer elicited overediting of the canonical miR-3144-3p to induce MSI2-dependent MET signaling in liver cancer.

miR-3144-3P overediting induces MSI2 and concomitantly suppressed SLC38A4 in liver cancer

Given we found that canonical miR-3144-3p overediting by ADAR1 contributed to malignant behavior in liver cancer cells, *in vitro* hepatocyte tumorigenesis experiments were performed to elucidate the tumor suppressive role of the canonical miR-3144-3p in liver cancer. Ectopic expression of a canonical miR-3144-3p mimic significantly repressed both tumor cell growth and proliferation of liver cancer cell, and MSI2 knock-down exhibited similar effects on the same cells (Fig. 5. A-C). Both canonical expression of miR-3144-3p and MSI2 knock-down were also associated with G1/S phase arrest of the liver cancer cells in flow cytometry analyses of PI-stained liver cancer cells (Fig. 5. D). In addition, canonical expression of miR-3144-3p and MSI2 knock-down significantly suppressed not only wound-healing efficacy, but also the migratory and invasive potential of the liver cancer cells (Fig. 5. E, F).

The editing product of the canonical miR-3144-3p, ED_miR-3144(3_A < G), is a novel and non-annotated miRNA. Therefore, it is important to elucidate the functional roles of ED_miR-3144(3_A < G) in liver cancer. Our analyses indicated ED_miR-3144(3_A < G) is produced during the process of liver cancer, and as a miRNA, it is considered to have a tumor suppressive function in the liver cancer process because it inhibits the translation of mRNA of a specific gene. To prove this hypothesis, we measured cell growth and differentiation rates after expressing active ADAR1 (pcDNA3.1_ADAR1-p110) or ED_miR-3144(3_A < G) mimic in liver cancer cells with low ADAR1 expression. Ectopic expression of either the ADAR1 or ED_miR-3144(3_A < G) mimics significantly augmented cell growth and proliferation rates of the liver cells (Fig. 6A). Next, we aimed to confirm our finding that the potential target of ED_miR-3144(3_A < G) was SLC38A4 in the liver cancer cells. Ectopic expression of an ED_miR-3144(3_A < G) mimic suppressed SLC38A4 protein expression, whereas an antisense ED_miR-3144(3_A < G) mimic rescued SLC38A4

expression in the liver cancer cells (Fig. 6B, upper). Note that a canonical miR-3144-3p mimic did not affect SLC38A4 protein expression (Fig. 6B, middle), and similar results were also obtained from the luciferase assay in the same cells (Fig. 6B lower). Luciferase assay showed binding ability of ED_miR-3144(3_A < G) to SLC38A4 3'-UTR respectively. In addition, ectopic expression of a primary mir-3144 mimic suppressed SLC38A4 protein expression, whereas co-transfection of ADAR1 siRNA rescued SLC38A4 expression in the liver cancer cells (Fig. 6C). After transfection of a plasmid expressing SLC38A4 without 3'-UTR, and then transfection with an ED_miR-3144(3_A < G) mimic, we found that only endogenous SLC38A4 was selectively suppressed, whereas SLC38A4 siRNA transfection inhibited endogenous and ectopic SLC38A4, implying selective regulation of SLC38A4 by ED_miR-3144(3_A < G) in liver cancer cells (Fig. 6D). These results were confirmed by the finding that SLC38A4 was inhibited when primary mir-3144 was co-transfected with pcDNA3.1-ADAR1-p110, whereas the pcDNA3.1-ADAR1-p110 mutant form was not. (Fig. 6E). These results showed that editing of the canonical miR-3144-3p by ADAR1 caused target-off for MSI2, and conversely, the newly created ED_miR-3144(3_A < G) inhibited a new target, SLC38A4, and thus contributed to liver cancer.

In vivo **functional validation of ADAR1, MSI2 and SLC38A4 in liver cancer**

Next, to demonstrate whether individual modulation of ADAR1, MSI2 and SLC38A4 affects liver tumorigenesis *in vivo*, we prepared H-*ras*-transgenic mice that spontaneously develop liver cancer beginning at approximately 14 weeks of age.[13] To investigate the cancer-preventive effect of targeting Adar1 and Msi2, or re-expressing Slc38a4 *in vivo*, mice were administered the liver-specific delivery reagents Invivofectamine (siAdar1 and siMsi2), and Turbofect (pcDNA3.1_Slc38a4) intravenously once weekly from 14 weeks of age (Fig. 7A, upper). Liver tumor masses were detectable at 21 weeks of age in the negative control group (N.C), in which 3 of 4 mice developed large and multiple tumor masses, whereas tumor masses from the siAdar1, siMsi2 and pcDNA3.1_Slc38a4 groups were relatively fewer and smaller than in the control group (Fig. 7A, lower). In addition, the incidence of mouse liver tumors in the negative control group was much greater than in the siAdar1, siMsi2 or pcDNA3.1_Slc38a4 groups (Fig. 7B). Total liver weight changes were also consistent with the remarkable inhibitory effect of targeting both Adar1 and Msi2, or re-expressing Slc38a4 with regard to the tumor load *in vivo* (Fig. 7C). Western blot analyses confirmed modulation of the expression of Adar1, Msi2 and Slc38a4 in the non-cancerous liver tissues surrounding tumor masses. And also, Met expression was repressed in the livers of the siMsi2-treated mice, showing a downstream effect of Msi2 on Met in liver cancer *in vivo* (Fig. 7D).

Discussion

Over the past few years, novel post-transcriptional regulatory mechanisms of action for miRNAs, including miRNA editing and chemical modifications, have been characterized and found to have an important role in cancer.[19] In particular, A-to-I editing of RNA has recently emerged as an important mechanism in cancer biology, being a widespread posttranscriptional process that increases various types of proteins and diverse functions from a limited set of genes. In addition to A-to-I editing of messenger RNA, some miRNA precursors undergo A-to-I editing, which regulates the expression and/or

function of mature miRNAs. For example, A-to-I editing within the recognition site for microprocessors such as DROSHA, DGCR8 and DICER may interfere with the biogenesis of mature miRNA[20] or alter the recognition of the target mRNA, particularly if editing occurs within the seed sequence of the miRNA. Thus, editing may transform certain tumor-suppressor miRNAs into oncogenic miRNAs.[7] In this study, miR-3144-3p was found to be closely associated with liver cancer after performing editing event, frequency and hotspot analyses using multi-stage liver cancer RNA genome data. Through functional analyses, overediting of the canonical miR-3144-3p was found to induce the MSI2 expression, and at the same time, ED_miR-3144(3_A < G) generated by editing of the canonical miR-3144-3p inhibited SLC38A4, providing correlations of miR-3144-3p editing with molecular drivers and signaling pathways in liver cancer.

A previous study of RNA editing hotspots in miRNAs across cancer types suggested 19 ADAR-dependent A-to-I RNA-editing hot spots in the mature sequence of miRNAs including miR-3144-3p.[7] The researchers focused on miR-200b, and showed the edited miR-200b promoted cell invasion and migration through its impaired ability to inhibit *ZEB1/ZEB2* and acquired ability to repress new targets *LIFR*, a metastatic suppressor. Our investigation also identified miR-3144-3p as a liver-cancer-specific ADAR1-dependent edited miRNA, with the adenine at position 3 of miR-3144-3p as an editing hotspot (Supplementary Figure S3). In addition, we found a frequent miR-200b editing event at position 5 of mature miRNA, as reported in a previous study of liver cancer. However, there was no significant change in the expression of miR-200b in liver cancer compared with normal tissues, whereas the expression of miR-3144-3p was increased about 20-fold or more in liver cancer (data not shown). In addition, our results showed that the frequency of miR-3144-3p editing increased liver cancer progressed, accompanied by an increased in the gene copy number of the corresponding loci, implying that miRNA editing contributes to liver cancer pathology.

Dysregulation of miR-3144-3p was first reported in human liver cancer, but few functional studies have been completed to date.[21] Musashi (MSI) RNA-binding proteins were originally found to regulate asymmetric cell division during embryonic development, and many studies have reported that MSI2 is tightly associated with advanced clinical stages of several cancers including liver cancer, but the signaling pathways that regulate MSI2 expression are currently unknown.[18] Also, even though the MSI2 target genes, such as MYC, LIN28A and MET, are well studied, the upstream overexpression mechanism of MSI2 was elusive in liver cancer development. Our data demonstrated that the canonical miR-3144-3p plays a role in regulating translation of *MSI2* mRNA in normal hepatocytes, although over-editing of the canonical miR-3144-3p is induced by aberrant regulation and activity of ADAR1. We also found that the loss of miR-3144-3p induces MSI2 overexpression, and contributes to liver cancer.

The solute carrier proteins (SLC) superfamily member SLC38A4 is a system A amino acid transporter. System A is a ubiquitous Na^+-dependent transporter that converts zwitterionic amino acids into N-methylated amino acids, such as alanine, serine and glutamine.[22] Amino acids are required for the survival and growth of highly proliferative cells such as embryonic cells and cancer cells. However,

SLC38A4 has been reported to function as a tumor suppressor in liver cancer through modulation of the Wnt/β-catenin/MYC/HMGCS2 axis.[23] Our analyses also showed down-regulation of SLC38A4 in large cohorts of liver cancer patients (Supplementary data, Table S3). In addition, Kaplan-Meier survival analyses of a large cohort of liver cancer patients (TCGA_LIHC) showed that the 5-year overall survival rate of liver cancer patients with low expression of SLC38A4 was significantly lower than that of the patients with high expression (data not shown). Transfection with a Slc38a4 expression plasmid significantly suppressed the tumorigenicity of a H-*ras* transgenic mouse liver cancer model. (Fig. 7A, B). Together, these findings indicate the SLC38A4 tumor suppressor is inhibited by ED_miR-3144(3_A < G) generated by ADAR1-dependent miR-3144-3p overediting, and that these effects contribute to malignant transformation and growth of liver cancer cells.

Our results demonstrate that ADAR1-dependent overediting of the canonical miR-3144-3p plays a pivotal role in the development and progression of liver cancer. Maintaining the normal activity and expression of ADAR1 appears to be important in maintaining the balance of canonical miRNAs that function as mitogenic signals in hepatocytes. Aberrant overexpression of ADAR1 induces editing of the canonical miR-3144-3p to induce translation of the oncogenic *MSI2* gene, thereby augmenting the growth, proliferation, motility and invasive potential of hepatocytes. In addition, ADAR1-dependent over-editing of the canonical miR-3144-3p creates a novel ED_miR-3144(3_A < G) that specifically suppresses *SLC38A4* mRNA translation to inactivate the tumor suppressor function of SLC38A4 during liver cancer (Fig. 7E). Together, these findings define a central role for ADAR1-dependent miR-3144-3p editing in liver cancer and suggest its potential therapeutic value for the treatment of liver cancer.

Declarations

ACKNOWLEDGEMENTS

This study was supported by grants from the National Research Foundation (NRF) of Korea (2021M3E5E7021893). The results shown in this study are in part based on data generated by the TCGA Research Network: http://www.cancer.gov/tcga.

AUTHORS CONTRIBUTIONS

HSK, MJN and SWN designed experiments and analyzed results. HSK and MJN performed the experiments. HDY, SYK, ES, JWH, SJ, KM, WSP provide support with experimental materials, techniques and data analysis. KHS and KK performed bioinformatics analysis. SWN supervised the study. All authors read and approved the final manuscript.

COMPETING INTERESTS

The authors declare no competing interests.

CONFLICT OF INTEREST STATEMENT

SWN is the chief execute officer of NEORNAT, Inc. HDY, SYK and KM are employee of NEORNAT, Inc. The other authors declare no conflict of interest relating to this work.

References

1. Keegan, L. P., Gallo, A. & O'Connell, M. A. The many roles of an RNA editor. Nat Rev Genet **2**, 869–878 (2001).
2. Bass, B. L. RNA editing by adenosine deaminases that act on RNA. Annu Rev Biochem **71**, 817–846 (2002).
3. Avesson, L. & Barry, G. The emerging role of RNA and DNA editing in cancer. Biochim Biophys Acta **1845**, 308–316 (2014).
4. Tan, M. H. *et al.* Dynamic landscape and regulation of RNA editing in mammals. Nature **550**, 249–254 (2017).
5. Han, L. *et al.* The Genomic Landscape and Clinical Relevance of A-to-I RNA Editing in Human Cancers. Cancer Cell **28**, 515–528 (2015).
6. Baysal, B. E., Sharma, S., Hashemikhabir, S. & Janga, S. C. RNA Editing in Pathogenesis of Cancer. Cancer Res **77**, 3733–3739 (2017).
7. Wang, Y. *et al.* Systematic characterization of A-to-I RNA editing hotspots in microRNAs across human cancers. Genome Res **27**, 1112–1125 (2017).
8. Ha, M. & Kim, V. N. Regulation of microRNA biogenesis. Nat Rev Mol Cell Biol **15**, 509–524 (2014).
9. Negi, V. *et al.* Altered expression and editing of miRNA-100 regulates iTreg differentiation. Nucleic Acids Res **43**, 8057–8065 (2015).
10. Shoshan, E. *et al.* Reduced adenosine-to-inosine miR-455-5p editing promotes melanoma growth and metastasis. Nat Cell Biol **17**, 311–321 (2015).
11. Ramirez-Moya, J., Baker, A. R., Slack, F. J. & Santisteban, P. ADAR1-mediated RNA editing is a novel oncogenic process in thyroid cancer and regulates miR-200 activity. Oncogene **39**, 3738–3753 (2020).
12. Chen, L. *et al.* Recoding RNA editing of AZIN1 predisposes to hepatocellular carcinoma. Nat Med **19**, 209–216 (2013).
13. Wang, A. G. *et al.* Gender-dependent hepatic alterations in H-ras12V transgenic mice. J Hepatol **43**, 836–844 (2005).
14. Futschik, M. E. & Carlisle, B. Noise-robust soft clustering of gene expression time-course data. J Bioinform Comput Biol **3**, 965–988 (2005).
15. Bazak, L. *et al.* A-to-I RNA editing occurs at over a hundred million genomic sites, located in a majority of human genes. Genome Res **24**, 365–376 (2014).
16. Shen, Q. *et al.* Barrier to autointegration factor 1, procollagen-lysine, 2-oxoglutarate 5-dioxygenase 3, and splicing factor 3b subunit 4 as early-stage cancer decision markers and drivers of hepatocellular carcinoma. Hepatology **67**, 1360–1377 (2018).

17. Chan, T. H. *et al.* A disrupted RNA editing balance mediated by ADARs (Adenosine DeAminases that act on RNA) in human hepatocellular carcinoma. Gut **63**, 832–843 (2014).
18. Kudinov, A. E., Karanicolas, J., Golemis, E. A. & Boumber, Y. Musashi RNA-Binding Proteins as Cancer Drivers and Novel Therapeutic Targets. Clin Cancer Res **23**, 2143–2153 (2017).
19. Torsin, L. I. *et al.* Editing and Chemical Modifications on Non-Coding RNAs in Cancer: A New Tale with Clinical Significance. Int J Mol Sci **22** (2021).
20. Nemlich, Y. *et al.* MicroRNA-mediated loss of ADAR1 in metastatic melanoma promotes tumor growth. J Clin Invest **123**, 2703–2718 (2013).
21. Wojcicka, A. *et al.* Next generation sequencing reveals microRNA isoforms in liver cirrhosis and hepatocellular carcinoma. Int J Biochem Cell Biol **53**, 208–217 (2014).
22. Shi, Q., Padmanabhan, R., Villegas, C. J., Gu, S. & Jiang, J. X. Membrane topological structure of neutral system N/A amino acid transporter 4 (SNAT4) protein. J Biol Chem **286**, 38086–38094 (2011).
23. Li, J. *et al.* SLC38A4 functions as a tumour suppressor in hepatocellular carcinoma through modulating Wnt/beta-catenin/MYC/HMGCS2 axis. Br J Cancer **125**, 865–876 (2021).

Figures

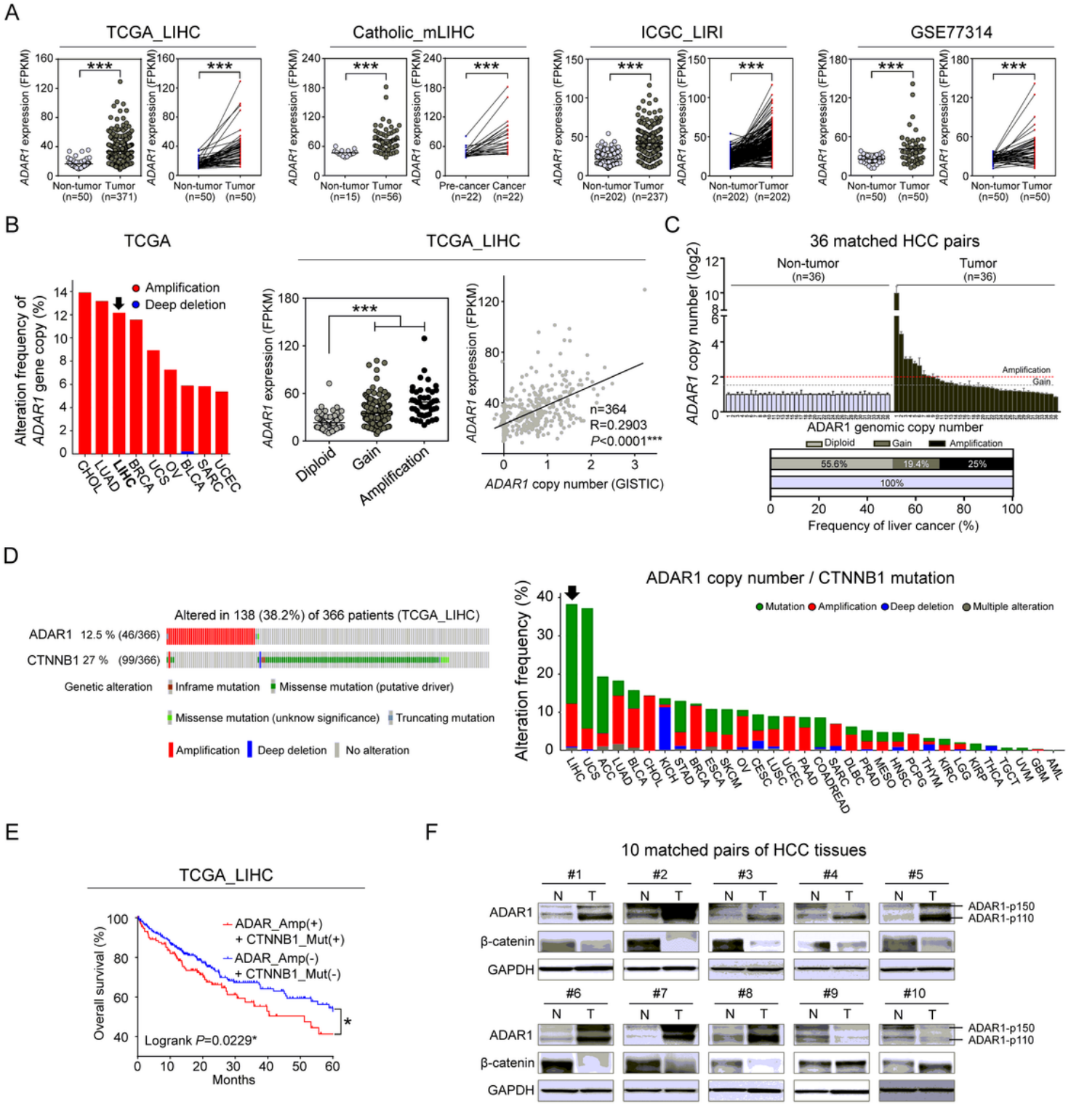

Figure 1

ADAR1 is overexpressed by the genomic amplification and its alteration is mutually exclusive with _CTNNB1_mutation in liver cancer.

A Differential gene expression of *ADAR1* in RNA-seq datasets of liver cancer patients compared with healthy normal patients (Non-tumor) and matched pairs of liver cancers. **B** *ADAR1* genomic alteration in

various cancers from cBioPortal (left). *ADAR1* expression change by genomic alteration from TCGA_LIHC data set (middle). The correlation of *ADAR1* gene expression with its genomic copy number value from TCGA_LIHC dataset (right). **C** qRT-PCR analysis of *ADAR1* gene copy number in matched human liver cancer tissues. **D** Oncoprint of genomic alteration with *ADAR1* and *CTNNB1* in liver cancer patients from TCGA_LIHC dataset. Mutual exclusivity analysis between *ADAR1* amplification and *CTNNB1* mutation (left). The systemic analysis of the merged alteration frequency of *ADAR1* and *CTNNB1*in TCGA dataset (right). **E** Kaplan-Meier survival curves with *ADAR1*gene amplification (Amp) and *CTNNB1* mutation (Mut) in liver cancer patients. **F** Western blot analysis of ADAR1 and β-catenin in 10 selected matched pairs of tumor (T) with adjacent non-tumor (N) tissues from liver cancer patients. All data are shown as the mean ±SEM. **P* < 0.05, ***P* < 0.01, ****P* < 0.001 by unpaired student's *t* test.

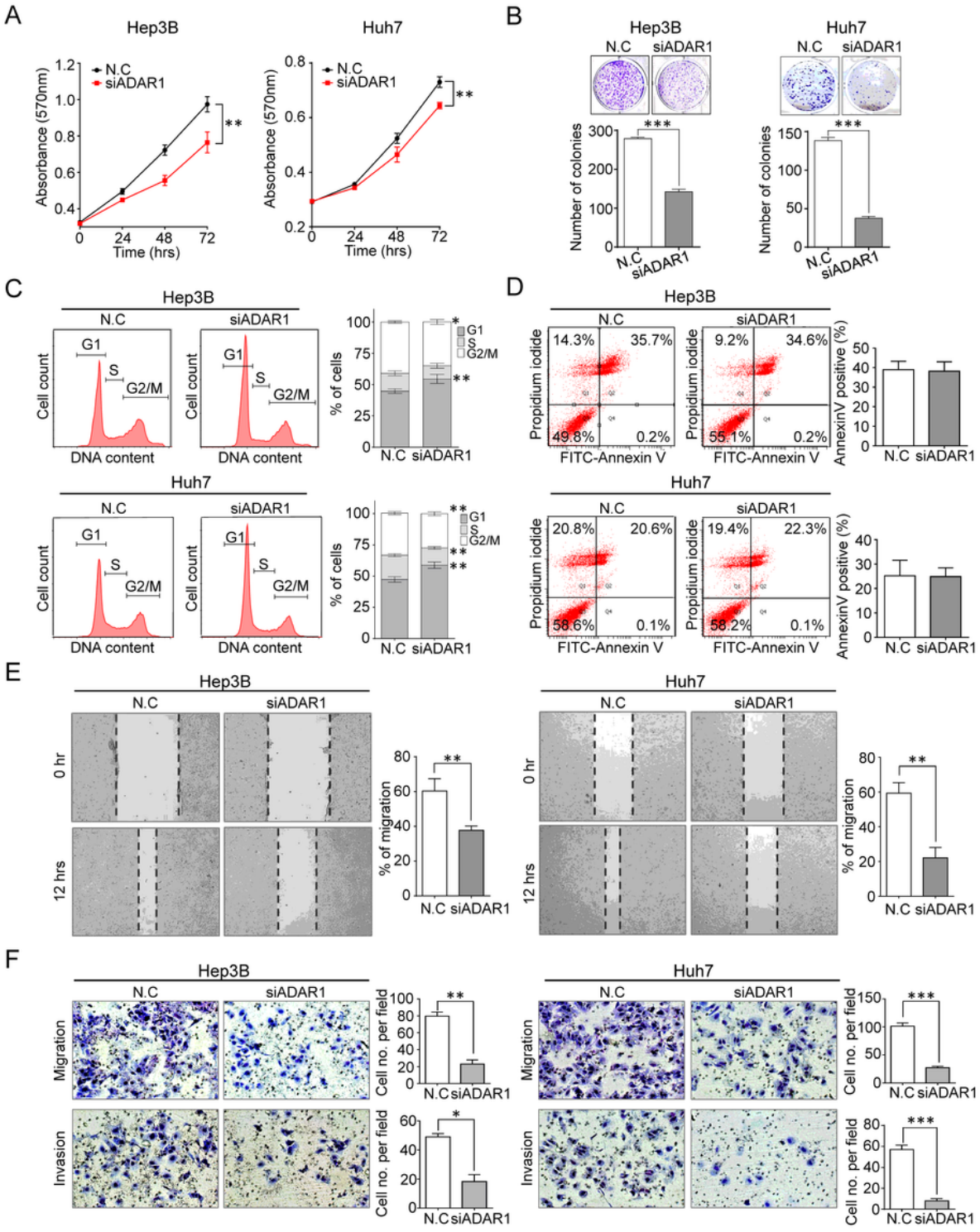

Figure 2

Targeted-inactivation of ADAR1 suppresses tumorigenic potential of liver cancer.

A Cell growth assay was measured by MTT. **B** Anchorage-independent growth was determined by clonogenic assay. **C** Flow cytometry of propidium iodide (PI) positive cells after treatment of control siRNA (N.C.) and ADAR1-specific siRNA (siADAR1), respectively (left). The PI-stained cell number ratios

are presented with bar graph (right). **D** The apoptosis rates of the cancer cells, stained with annexin V-FITC and propidium iodide, were evaluated with flow cytometry after ADAR1 knockdown (left). The annexin V-FITC stained cell ratios are presented with bar graph (right). **E** Scratch wound healing assay (left), and the ratios of the remaining gap were represented with bar graph (right). **F**Transwell migration and invasion assays. All data are shown as the mean ± SEM. **P* < 0.05, ***P* < 0.01, ****P* < 0.001 by unpaired student's *t* test.

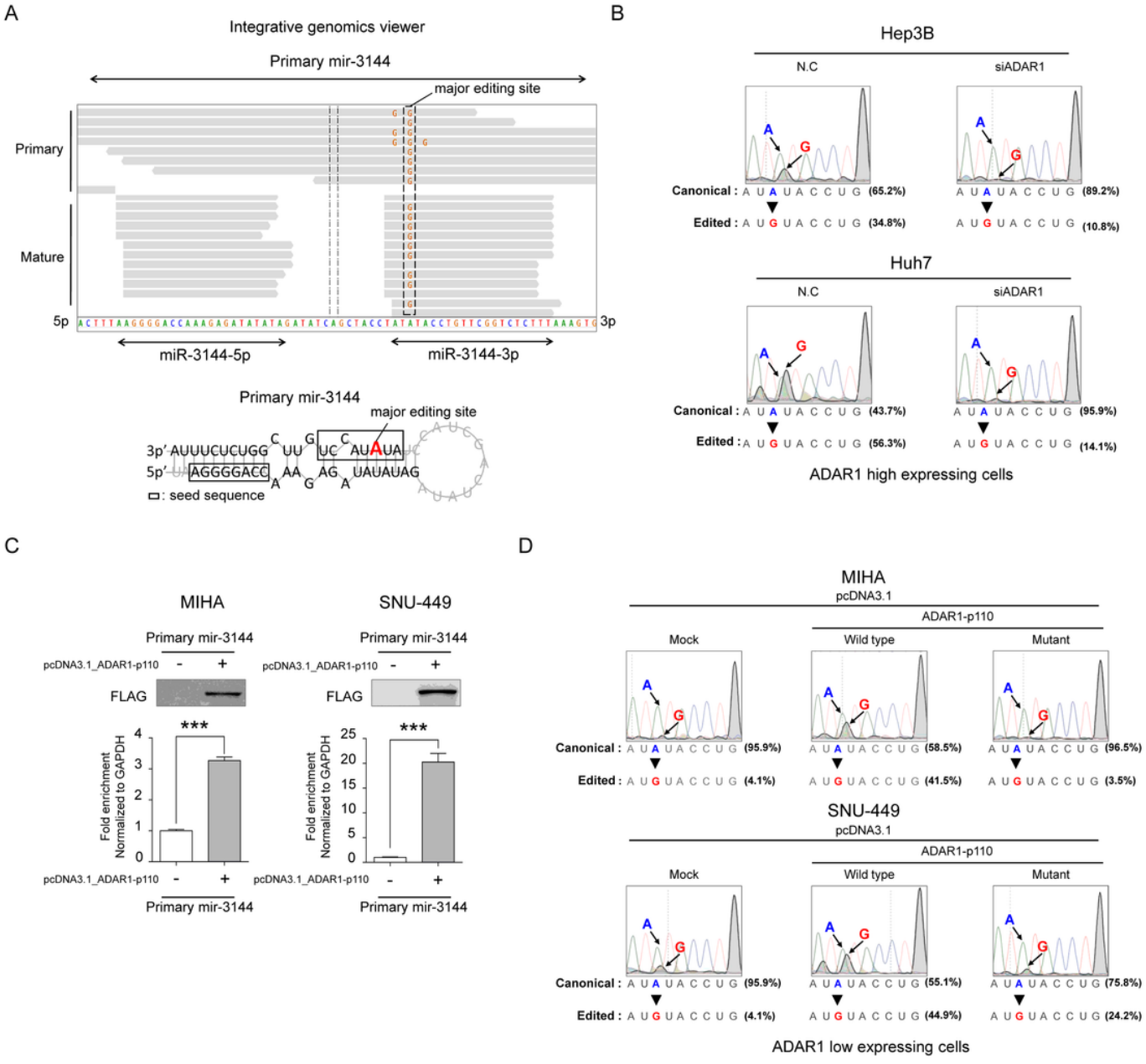

Figure 3

ADAR1-dependent A-to-I editing of canonical miR-3144-3p in liver cancer.

A Representative integrative genomics viewer (IGV) image of A-to-I editing sites in primary mir-3144 (upper) sequence and seed region of mature miR-3144 (lower) in liver cancer patients. Red color indicates

a major editing site of precursor mir-3144. **B** Direct sequencing analyses after ADAR1 knockdown in ADAR1 high expressing liver cancer cell lines. **C** RNA immunoprecipitation assay in ADAR1 overexpressing cells. The fold enrichment of primary mir-3144 was measured by qRT-PCR and normalized to GAPDH. **D** Direct sequencing analyses of miR-3144-3p in wild type or mutant ADAR1 overexpressing cells. All data are shown as the mean ± SEM. *$P < 0.05$, ***$P < 0.001$ by unpaired student's *t* test.

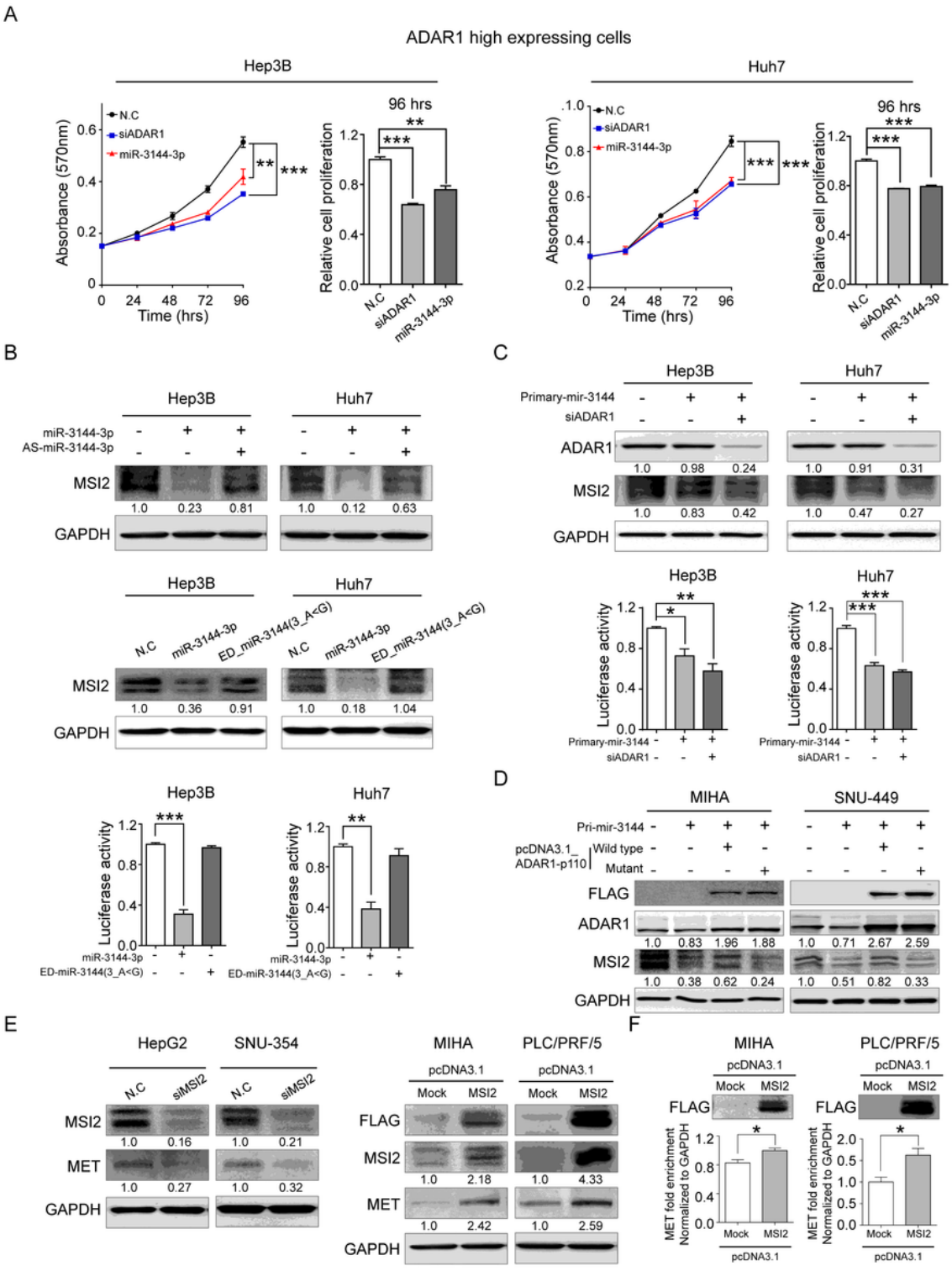

Figure 4

Activation of oncogenic MSI2 by ADAR1-dependent editing of canonical miR-3144-3p in liver cancer.

A ADAR1 knock-down and miR-3144-3p suppress liver cancer growth, determined by using MTT assay. **B** Antisense miR-3144-3p (upper), but not ED_miR-3144(3_A<G) mimics, attenuated suppression of MSI2 by canonical miR-3144-3p in liver cancer cells (middle and lower). **C** Western blot (upper) and luciferase reporter assay (lower) showed MSI2 regulation by ADAR1-dependent primary mir-3144 editing in liver cancercells. **D** ADAR1-dependent MSI2 expression was subjected to immunoblot analysis. **E** Western blot was performed in the condition of MSI2 knockdown (left) or ectopic overexpression of pcDNA3.1-MSI2 (right). **F** MET transcript was pulled down with pcDNA3.1-MSI2 and the enrichment of MET was measured by qRT-PCR. All data are shown as the mean ± SEM. *P < 0.05, **P < 0.01, ***P < 0.001 by unpaired student's t test.

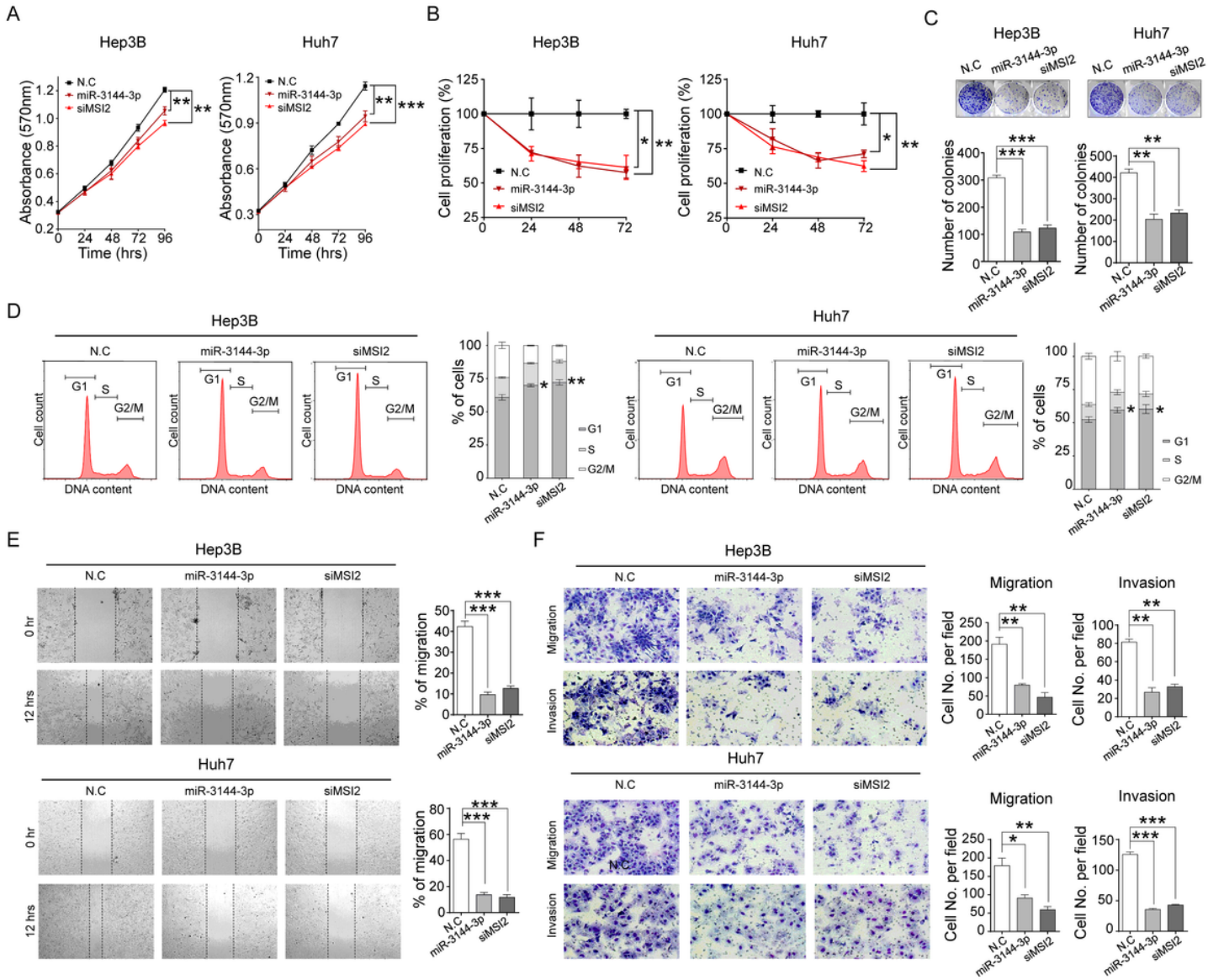

Figure 5

ADAR1-dependent canonical miR-3144-3p editing contributes tumorigenic potential of liver cancer.

To assess anti-tumorigenic effect of miR-3144-3p and MSI2 in liver cancer cells, MTT **A**, BrdU **B** and clonogenic assays **C** were performed in miR-3144-3p mimics or MSI2 siRNA (siMSI2) treated cells. **D** DNA content of PI-stained cells was analyzed by flow cytometry. The stained cell number ratios are presented in bar graph. **E** Representative cell image (left) and migration percentage (right) of cells measured by scratch wound healing assay. **F** Transwell migration and invasion assays. All data are shown as the mean ± SEM. *P< 0.05, **P < 0.01, ***P < 0.001 by unpaired student's t test.

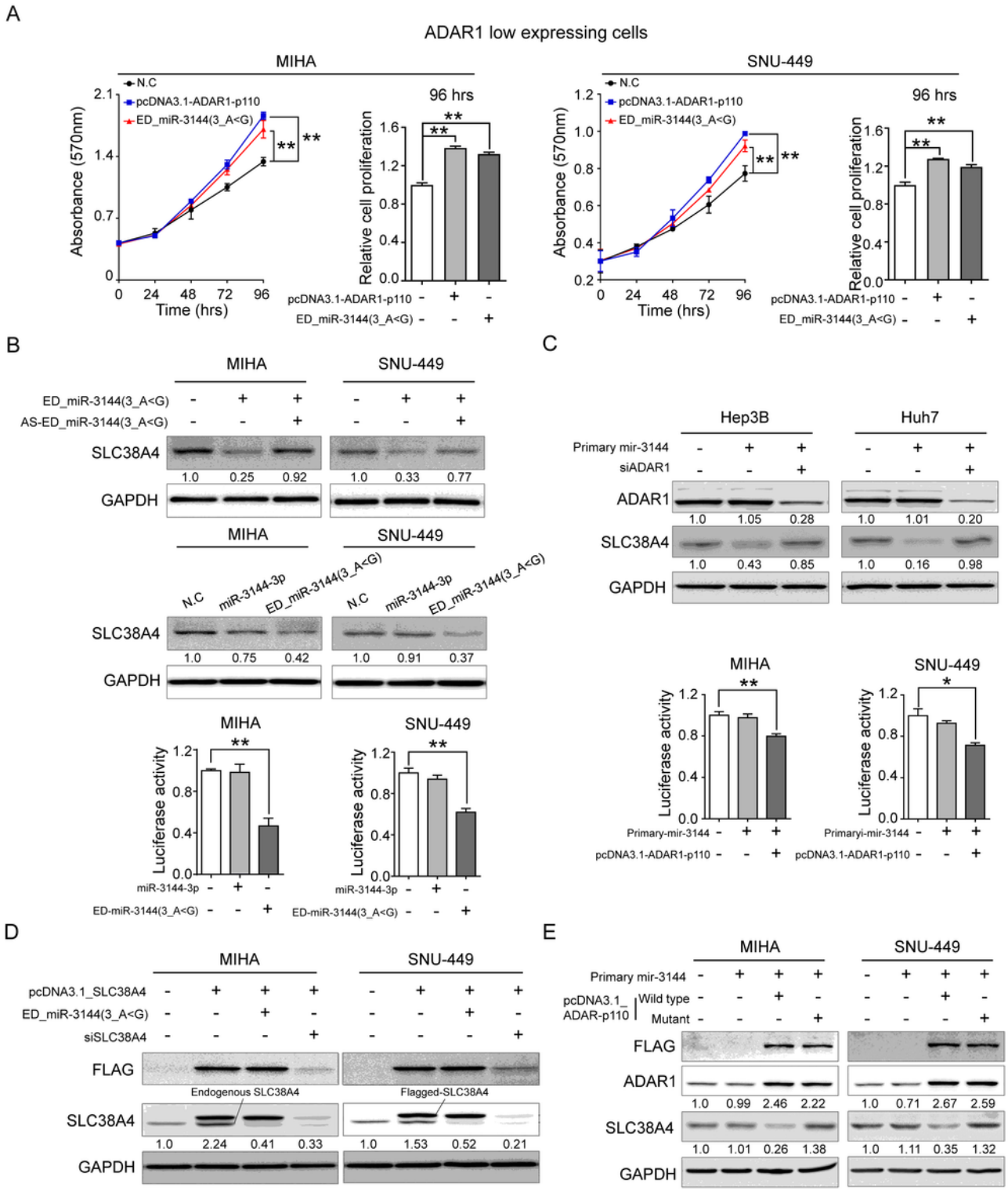

Figure 6

ED_miR-3144(3_A<G) functions as onco-miR in liver cancer.

A Cell growth was measured by MTT assay after transfection. **B** Cells were transfected with ED_miR-3144(3_A<G) mimics or co-transfected with antisense ED_miR-3144(3_A<G) (AS-ED_miR-3144(3_A<G)) (upper). miR-3144-3p or ED_miR-3144(3_A<G) mimics is ectopically transfected to cells (middle). Western

blot (middle) and luciferase reporter assay (lower). **C** Western blot was performed after transfection of primary mir-3144 or co-transfected with siADAR1 into Hep3B and Huh7 cells (upper). Luciferase reporter assay was performed in MIHA and SNU-449 cells (lower). **D**Western blot analysis shows direct regulation of ED_miR-3144(3_A<G) on SLC38A4 expression. **E** Cells were co-transfected with wild type or mutant expressing pcDNA3.1_SLC38A4 with primary mir-3144. All data are shown as the mean ± SEM. *P < 0.05, **P < 0.01 by unpaired student's t test.

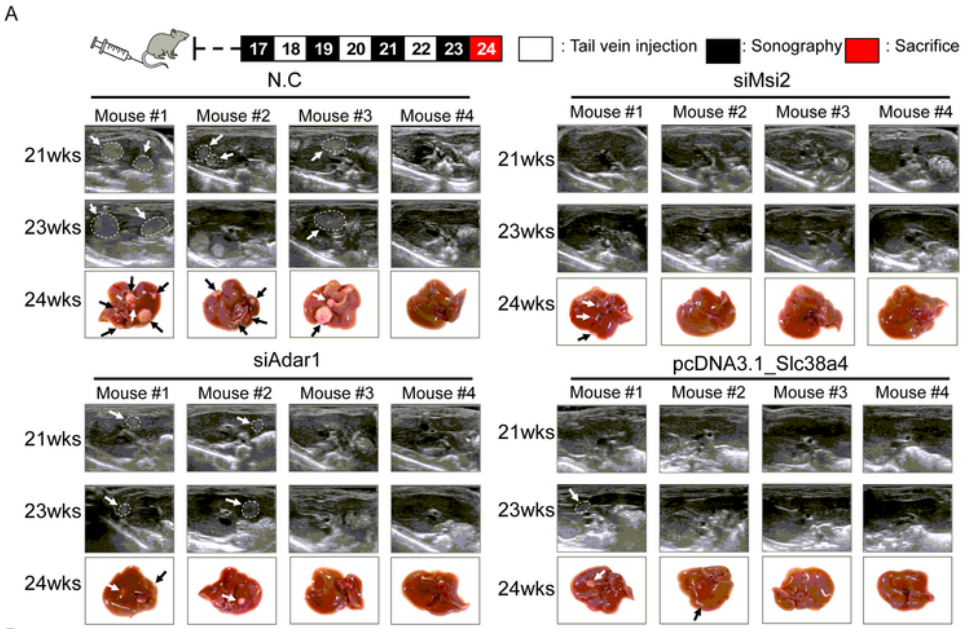

B

No.	Group	Mouse #	Number of tumor masses			
			19wks	21wks	23wks	24wks
1	N.C	#1		1	3	6
		#2		2	3	4
		#3		1	1	2
		#4				
2	siAdar1	#1		1	1	2
		#2		1	1	1
		#3				
		#4				
3	siMsi2	#1				3
		#2				
		#3				
		#4				
4	pcDNA3.1_Slc 38a4	#1			1	1
		#2				1
		#3				
		#4				

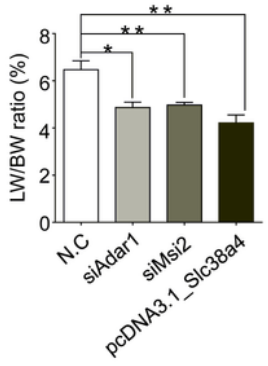

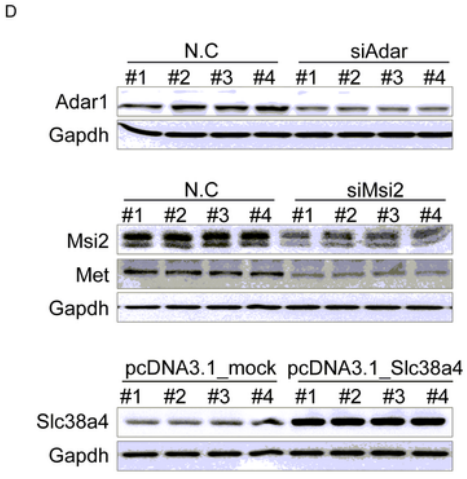

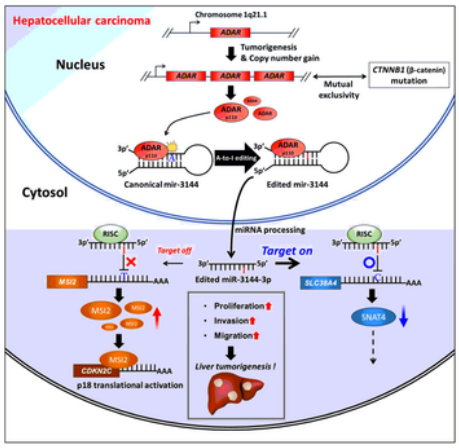

Figure 7

***In vivo*validation of ADAR1, MSI2 and SLC38A4 in mouse.**

A Timeline of *In vivo* transfection of siAdar1, siMsi2 and pcDNA3.1_Slc38a4 in H-*ras*-transgenic mouse model (upper). Representative ultrasonography images of mouse liver cancer model at 21 and 23 weeks of age, respectively, and liver images were taken at 24 weeks of age (lower). **B** The tumor mass numbers of each mouse at indicated weeks of age are listed in table. **C**Bar chart showing liver weight (LW) and body weight (BW) ratio (%) in each group. **D** Western blot analysis of Adar1, Msi2, Met and Slc38a4 expression in H-*ras*-transgenic mice. Gapdh is used for loading control. All data are shown as the mean ± SEM. *$P < 0.05$, **$P < 0.01$ by unpaired student's *t* test. **E** Schematic summary of miR-3144-3p target-on and -off mechanism induced by A-to-I RNA editing of up-regulated ADAR1-p110 in liver cancer development.

Supplementary Files

This is a list of supplementary files associated with this preprint. Click to download.

- Supplementarydata.docx